DETERMINATION OF CRYSTALLINITY IN POLYETHYLENE FROM ^{1}H-NMR FID ANALYSIS EFFECT OF NON-CURIE TEMPERATURE BEHAVIOUR

Eddy Walther Hansen & Jaan Roots

Department of Chemistry, UiO, P.O. Box 1033 Blindern, N-0315 Oslo, Norway.
E-mail: eddywh@kjemi.uio.no

ABSTRACT

Hansen and coworkers (Zhang, L; Hansen, E. W.; Helland, I; Hinrichsen, E.; Larsen, Aa.; Roots, J. *Macromolecules*, **2009**, 42 (14), 5189-5195) recently reported on the room temperature crystallinity of a series of ethene-1-hexene copolymers using solid-state ^{1}H-NMR FID analysis. However, due to the required 10 μs blanking time of the receiver vital information in the initial part of the FID was lost resulting in an underestimation of the sample crystallinity. To compensate for this information loss we made use of the significant increase in T_2 at or above the melting point which enabled the intensity of the FID at time t = 0 to be reliably estimated. Hence, by applying the Curie law the room temperature intensity of the FID was re-evaluated and resulted in an improved crystallinity value. However, it was still too small compared to the crystallinity obtained by solid-state ^{13}C-NMR. However, by multiplying the proton FID intensity (determined at the melting point) by a factor of 1.25 before applying the Curie law, the room temperature crystallinity derived from the two different NMR techniques became – within experimental error – consistent. In this work we present experimental evidence that the empirical multiplication factor of 1.25 strictly originates from a non-Curie temperature behaviour of the NMR signal intensity.

Keywords*: LLDPE, ^{1}H-NMR, FID, Curie-law, Crystallinity.*

1. INTRODUCTION

From a phenomenological point of view, a semi-crystalline polymer can be considered to be composed of crystallites embedded in a non-crystalline (amorphous) matrix in which the mass-fraction or volume-fraction of crystallites define the crystallinity. Any experimental method sensitive to the difference in physical properties between the two domains constitutes a potential technique to probe crystallinity.

During the last decade various solid-state NMR techniques have been applied [1-4] to derive the crystallinity of semi-crystalline polymers. These experimental techniques are sensitive to differences in molecular dynamics and/or molecular structures. In particular, proton free-induction decay (^{1}H-FID) analysis has become increasingly popular as it combines the advantages of being sensitive, robust, fast and nearly independent of the magnetic field strength, and allows the adoption of less costly low-field NMR spectrometers.

However, the inherent noise in the initial part of the FID (as caused by rf-pulse breakthrough) calls for a time delay in the start of the acquisition and results in estimated crystallinites that are systematically smaller compared to the "true" crystallinity [5-9].

In a recent work [9] the "dead time"-effect was circumvented by acquiring a second FID of the sample at, or close to its melting temperature in order to estimate the FID intensity at room temperature by applying the well known Curie law. However, the derived crystallinity was still significantly smaller compared to the crystallinity derived from solid-state ^{13}C-NMR and was tentatively ascribed to a temperature dependence of the Q-factor of the probe. However, Q is expected to change substantially if the sample changed its dielectric permittivity or diamagnetic permeability. For a substantial effect, the sample would have to be severely dielectrically lossy. This is probably not the case for an unpolar polymer such as PE. Another source of temperature dependence could be other changes in the electronic circuit, such as thermal expansion of the coil or the capacitors and must be considered probe/spectrometer dependent, which is why the effect is not necessarily expected to be the same as in [9] (Bruker minispec) and the presently used Maran Ultra. However, from a more pragmatic point of view we have noticed that using a low field NMR instrument the signal intensity does not necessarily follow the expected Curie-temperature behaviour.

In the present work we will apply a solid-echo NMR technique, as discussed previously by Litvinov et. al. [10], to provide experimental evidence for this non-Curie behaviour of the signal intensity as a function of temperature.

2. EXPERIMENTAL

2.1 Samples.

In this work an ethene-1-hexene copolymer containing 3.85 mol% of 1-hexene is used. The sample was synthesized by Borealis AS, Norway, using a single-site (metallocene) catalyst and provided in powder. The sample was

stabilized with Irganox B220 (1000 ppm), which after careful homogenization was pressed into plates 50 mm x 50 mm x 2 mm (first kept at 220 ^{o}C for 3 min, then cooled at 40 ^{o}C/min to below 80 ^{o}C, and subsequently to 20 ^{o}C at a lower cooling rate). This sample is identical to sample F in ref [9].

2.2 NMR Measurement

All proton solid-echo experiments were performed on a low-field NMR spectrometer (Maran Ultra) operating at 0.5 Tesla. This same instrument was to acquire the ^{1}H-FIDs presented in [9]. The sample was placed in a 10 mm outer diameter NMR tube which fitted well within the volume of the transmitter/receiver coil. The spectrometer provided short 90^{o} pulses (2.15 μs) with reliable phase switching and fast digitizing (every 0.1 μs) with a required 10 μs dead time to overcome the break through of the rf-pulse. The temperature was digitally controlled with a stability better than $\pm$1˚C. All experiments were performed after a temperature stabilization of 10 minutes. The temperature was raised successively from room temperature T_R (= 296 K) to T = 311 K, 327 K, 343 K, 360 K, 377 K and 391 K at a rate of approximately 10^{0}C/min. The number of scans was set to 16 with a recycling delay of 5 s to ensure quantitative sampling of the signal.

3. FID-ANALYSIS

In this work we will assign the Free Induction Decay (FID) signal or any of its components by small letters. For instance, the ^{1}H-FID f(t) of a semi-crystalline polyethylene can be represented by a sum of two FID-components, a crystalline component $f_C(t)$ and an amorphous component $f_A(t)$ according to:

$$f(t) = \rho \cdot f_C(t) + [1-\rho] \cdot f_A(t), \quad \text{with} \quad 0 \le \rho \le 1 \tag{1a}$$

where ρ represents the crystallinity and $f_C(t)$ takes the form [11-18];

$$f_C(t) = \exp\left[-\frac{1}{2}(t/T_{2r})^2\right] \cdot \frac{\sin \omega t}{\omega t} \tag{1b}$$

where $1/T_{2r}$ and ω define the apparent spin-spin relaxation time and the circular frequency factor, respectively. Equation 1b was first suggested by Abragam [11]as a phenomenological expression of the ^{19}F FID of CaF_2 and is simply denoted the "Abragamian". This function has been shown to be a good representation of the FID from other, crystalline lattices. It is worth mentioning that a slightly modified version of Equation 1b has been reported [18] in which the power coefficient 2 was replaced by an adjustable parameter γ (having a value between 1 and 2) and characterizes rather well highly crystalline PE samples that were etched for a long time. However, this is a rather exceptional type of function and introduces simply an additional adjustable parameter in the fit.

Concerning the rather complex theoretical representation of the amorphous FID-component $f_A(t)$, as introduced by Brereton [19,20] it has been shown that it can be well approximated by a sum of a Weibullian function w(t) and one or two stretch exponential functions s(t) [17];

$$f_A(t) = \mu \cdot w(t) + [1-\mu] \cdot s(t) \quad \text{with} \quad 0 \le \mu \le 1 \tag{1c}$$

$$w(t) = \exp\left[-\left(\frac{t}{T_{2,m1}}\right)^{\alpha 1}\right] \quad \text{with} \quad 1 \le \alpha 1 \le 2 \tag{1d}$$

$$s(t) = \exp\left[-\left(\frac{t}{T_{2,m2}}\right)^{\alpha 2}\right] \quad \text{with} \quad 0 \le \alpha 2 \le 1 \tag{1e}$$

where the time parameters $T_{2,X}$ (X = m1 and m2) represent apparent spin-spin relaxation times and μ defines the relative fraction of the Weibullian contribution to $f_A(t)$.

Additional details regarding the application of Equations 1a-1e can be found in [9] in which the eight adjustable parameters ρ , μ , ω, α1, α2, T_{2r}, $T_{2,m1}$ and $T_{2,m2}$ were determined by model fitting.

3.1 Solid-echo analysis

In order to differentiate between a ^{1}H-FID and a solid echo decay we will use a capital letter F(t;τ) for the latter where the time parameter τ defines the time distance between the mid-points of the two successive 90^{0} rf-pulses. If the first sampling point of the solid-echo decay occurs a time $t' (\ge 2\tau)$ after the first rf-pulse we define a new time parameter $t = t' - 2\tau$ which results in maximum (echo) intensity at t = 0. In this work, τ is varied from 10 μs to 25 μs in steps of 1 μs implying that the extrapolated FID amplitude f(0) equals the maximum solid echo amplitude F(0;τ) at t = τ = 0.

In order to simplify equations and formulas presented in this work we will avoid complicated and unnecessary notations and thus exclude the temperature symbol T. This latter parameter will only be introduced explicitly when ambiguities may arise.

4. RESULTS AND DISCUSSION

Figure 1 shows four (out of 13 experiments) of the solid-echo decays $F(t;\tau)$ acquired at temperature T = 377 K with τ = 10.15 μs, 15.15 μs, 20.15 μs and 24.15 μs, respectively.

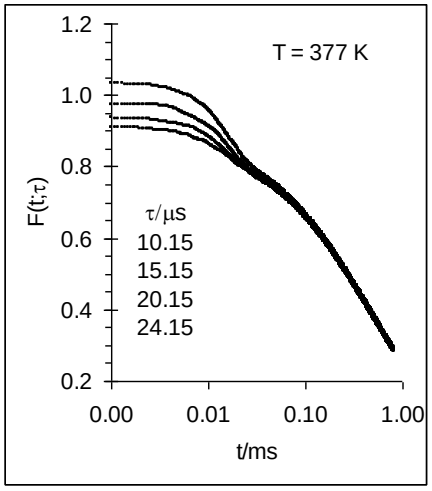

Figure 1. Solid-echo decay $F(t;\tau)$ acquired at temperature T = 377 K with τ = 10.15 μs, 15.15 μs, 20.15 μs and 24.15 μs, respectively. The signal intensity of the echo maximum appears at t = 0 and equals $F(0;\tau)$. The solid curves represent model fits to Equations 1a – 1e. See text for further details.

Figure 2 (top) illustrates a non-linear least squares fit of Equation 1a-1e to the solid echo decay $F(t;\tau)$ for T = 377 K and τ = 10.15 μs. As can be noted, the residual between the observed and model fitted echo decays is less than 0.5%. Importantly, the error distribution is practically random. Moreover, the stretch exponential function $S(t;\tau)$, which represents the signal intensity of the mobile amorphous component decays much slower than the rigid amorphous component $W(t;\tau)$ and reflects the much shorter T_2 (= T_{2m1}) of the latter component. The relatively small amplitude of $F_C(0;\tau)$ at this high temperature reveals a small crystallinity, as expected at this higher temperature.

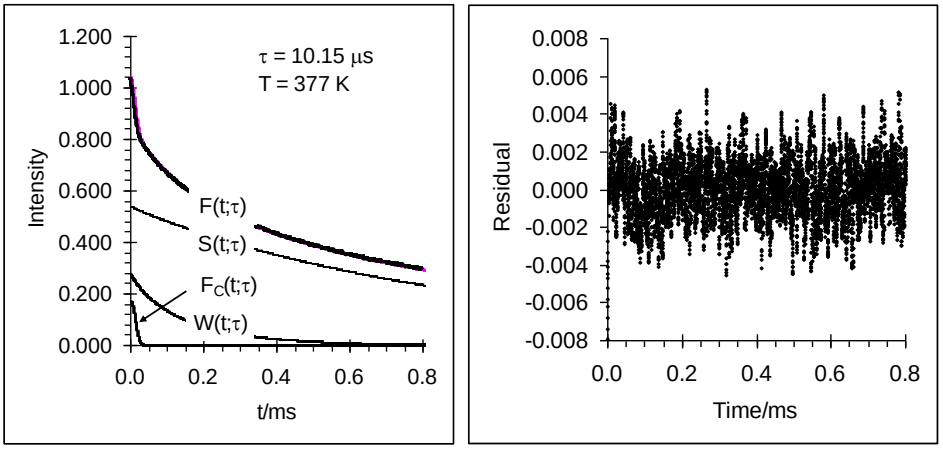

Figure 2. Top) The solid-echo signal intensity $F(t;\tau$ = 10.15 μs) at T = 377 K as a function of time t. The model fitted components $F_C(t;\tau)$, $W(t;\tau)$ and $S(t;\tau)$ were obtained by a non linear least squares fit to Equations 1a-1e. Bottom) The residual between model fitted and observed sold-echo signal $F(t;\tau$ =10.15 μs) as a function of time t.

Since the objective is to determine the FID intensity f(0) at time t = 0, we will be concerned about obtaining numerical value of $F_C(0;0)$, $F_A(0;0)$, $W_A(0;0)$, $S(0;0)$, ρ and μ by model fitting to Equations 1a -1e. The actual numerical value of the parameters ω, α1, α2, T_{2r}, $T_{2,m1}$ and $T_{2,m2}$ is of minor interest, and will not be reported. The analytical approach is illustrated on Figure 3.

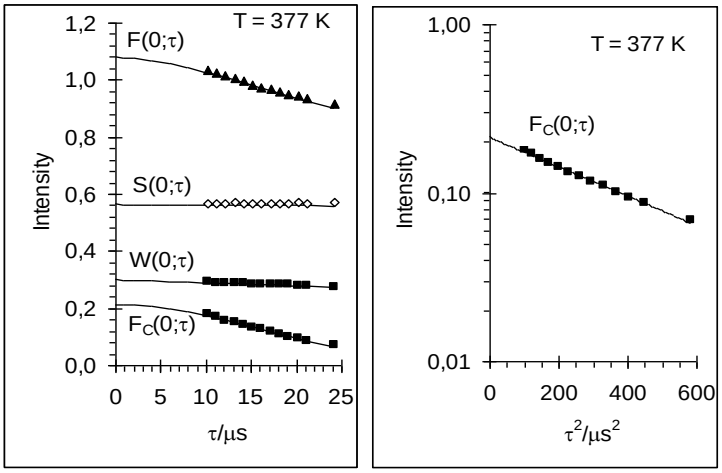

Figure 3. Left) Signal intensities $F(0;\tau)$, $F_C(0;\tau)$, $S(0;\tau)$ *and* $W(0;\tau)$ *as function of τ. The solid curves represent model fits to Equations 1a – 1e (with x(t) replaced by X(t; τ))), as described in the text. Right) The solid-echo amplitude of the crystalline component* $F_C(0;\tau)$ *as a function of the echo-time squared (τ²).*

Within the experimental τ-window ($10.15\mu s \le \tau \le 24.15\mu s$; Figure 3) both components $W(0;\tau)$ and $S(0;\tau)$ can be excellently approximated by straight lines. Hence, $W(0;0)$ and $S(0;0)$ can be easily determined. A corresponding linear behaviour is not observed for the crystalline solid-echo decay $F_C(0;\tau)$ and has been pointed out previously by Litvinov et al [10] who simply argued that $F_C(0;\tau)$ may be approximated by a linear function in τ for short τ-values, i.e., for $\tau/T_{2r} << 1$. The data presented in Figure 3 (right) suggests, however, that the observed echo-envelope of $F_C(0;\tau)$ is excellently characterized by a Gaussian function within the whole experimental τ-region. Actually, this Gaussian behaviour of $F_C(0;\tau)$ with respect to τ was found to be valid for all temperatures investigated in this work. An experimental and theoretical justification for this behaviour has been discussed by Boden and co-workers by introducing a so-called "loosely-coupled spin-1/2 pairs"-model [21,22]. As a consequence, $F_C(0;0)$ was determined by model fitting $F_C(0;\tau)$ to a Gaussian function with respect to τ for any temperature T. Based on the above arguments, the maximum echo amplitude $F(0;0)$ (= f(0)) was derived from Equation 3 by determining $F(0;\tau \to 0)$;

$$F(0;\tau) = \rho \cdot F_C(0;\tau) + (1-\rho) \cdot F_A(0;\tau) \qquad (3)$$

The results are summarized in Figure 4 in which the signal intensity F(0;0) (=f(0)) of the melted sample was arbitrary set to 1 and used as a reference.

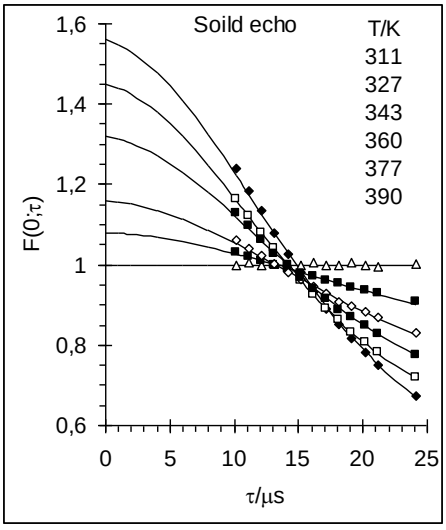

Figure 4. Solid echo amplitude F(0; τ) as a function of τ for different temperature T. For reference purposes the signal intensity F(0;0) at the melting temperature was set equal to 1. The solid curves were calculated by fitting $F_C(0;\tau)$ *to a Gaussian function with respect to τ, as discussed in the text.*

As can be inferred from the data in Figure 4, the echo envelope $F(0;\tau)$ at the melting temperature reveals an extremely slow decay rate which is approximately constant and independent on τ and signifies a much longer spin-spin relaxation time T_2 (as expected from the highly mobile molecular motion in the melt) compared to the corresponding T_2 of the non-melted sample. As pointed out previously and illustrated on Figure 4, the ^{1}H-FID intensity f(0) (= F(0;0)) at time t = 0 is actually a function of the absolute temperature T. Hence, we introduce the notation f(0:T) to symbolize the ^{1}H-FID intensity f(0) at any temperature T. Based on the data shown in Figure 4, the normalized ^{1}H-FID intensity $f(0;T)/f(0;T_M)$ is plotted as a function of the absolute temperature T (or more correctly, as a function of the inverse absolute temperature 1/T) and is depicted in Figure 5 (left), where $f(0;T_M)$ is the intensity of the sample at its melting temperature (T_M).

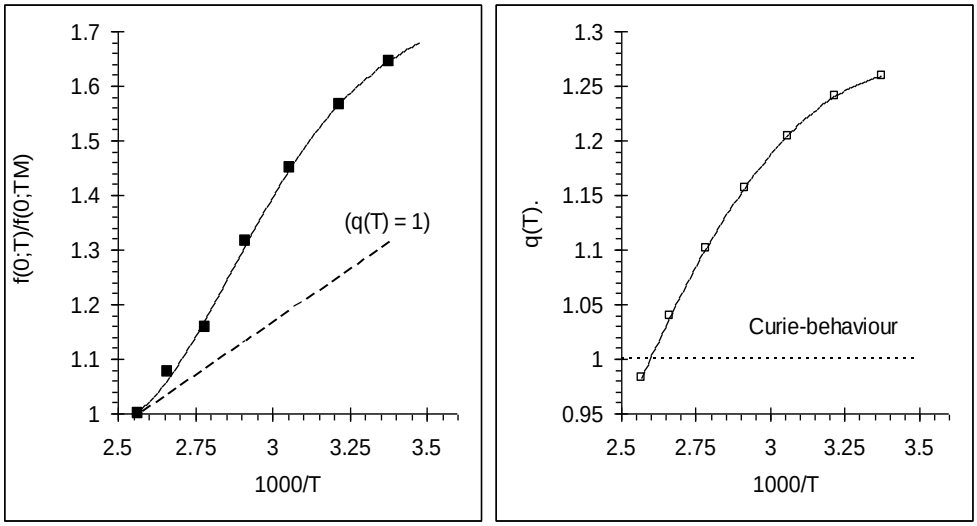

Figure 5. Left) The "observed" and normalized ^{1}H-FID intensity $f(0;T)/f(0;T_M)$ of the PE sample as a function of the inverse temperature (1/T; ■) where $f(0;T_M)$ is the intensity of the sample at its melting temperature T_M. The solid curve represents the best fit to a Boltzmann function. The dotted curve shows the temperature dependence of the ^{1}H-FID if it was exclusively determined by the Curie law, i.e., with q(T) = 1 (Equation 4).
Right) The actual dependence of the temperature correction term q(T) (Eq 4) is shown by the solid squares (□) in which the solid curve represents a best fit to a polynomial function. The dotted curve (q(T) = 1) represents the temperature correction term if the signal intensity f(0;T) was solely determined by the Curie-effect.

Of practical reasons we define the normalized FID intensity (at time t = 0) according to Eq 4:

$$\frac{f(0;T)}{f(0;T_M)} = q(T)\cdot\frac{T_M}{T} \qquad (4)$$

Where q(T) represents an unspecified temperature correction term. The observed intensity ratio $f(0;T)/f(0;T_M)$ is plotted as a function of the inverse absolute temperature 1/T in Figure 5 (left). According to the well known Curie law, this signal intensity ratio is theoretically expected to be proportional to 1/T (i.e., q(T) = 1 in Equation 4) and is illustrated by the dotted curve in Figure 5; left.
In a recent publication [9] the problem related to the so called "dead time" effect was circumvented by measure the ^{1}H-FID intensity $f(0;T_M)$ at the melting temperature and then estimating its corresponding intensity $f(0;T_R)$ at room temperature T_R by applying Equation 4 with q(T) = 1. However, the resulting ^{1}H-NMR crystallinity was found to be underestimated with respect to the crystallinity derived by solid-state ^{13}C-NMR [9]. Actually, it was noted (empirically) that the crystallinity derived from the two different NMR techniques became equal only if the ^{1}H-FID intensity at room temperature, was further multipled by a factor of 1.25.
This additional correction of the ^{1}H-FID intensity can be rationalized from the data presented in Figure 5 (right), which shows that a second temperature correction $q(T_R)$ of the ^{1}H-FID intensity at room temperature was needed. This second temperature correction term is tentatively explained by changes in sample properties and probe characteristics (Q-factor of the probe) with temperature, as discussed thoroughly in the literature [23-27].
From Figure 5 (right) we find that at T_R = 296 K, $q(T_R)$ equals 1.26 $\pm$ 0.03 and is in excellent agreement with the empirical correction factor of 1.25 used in [9].

5. CONCLUSION

In this work we have shown that if the ^{1}H-FID of a semi-crystalline polymer is hampered by a significant dead time of the probe, implying that the crystallinity can not be reliably determined from a ^{1}H-FID analysis without knowing the actual temperature dependence of the quality factor of the probe. This requires, however, a ^{1}H-FID measurement of the melted sample and implies that the NMR technique no longer is non-destructive, because the temperature history of the sample is lost during melting.

In conclusion, if the dead time of the NMR probe represents a severe problem in estimating accurately the FID intensity f(0;T) at temperature T, the solid-echo technique is the ultimate NMR approach when aiming at determining crystallinity. The price to pay, however, is an increasing overall experimental time.

However, the results obtained in this work suggest that the crystallinity of semi-crystalline polymers may be obtained by applying a two-point solid-echo technique, i.e., by acquiring solid-echo decays at only two different echo times, τ_1 and τ_2, respectively. Work is in progress to evaluate this approach in more details.

6. REFERENCES

[1] Asano, A.; Tanaka, C.; Murata, Y. *Polymer* **2007,** 48, (13), 3809-3816.
[2] Barendswaard, W.; Litvinov, V. M.; Souren, F.; Scherrenberg, R. L.; Gondard, C.; Colemonts, C. *Macromolecules* **1999,** 32, (1), 167-180.
[3] Thakur, K. A. M.; Kean, R. T.; Zupfer, J.M.; Buehler, N.U.; Doscotch, M.A.; Munson, E.J. *Macromolecules* **1996,** 29, (27), 8844-8851.
[4] Maus, A.; Hertlein, C.; Saalwaechter, K. *Macromol. Chem. Phys.* **2006,** 207, (13), 1150-1158.
[5] Bridges, B. J.; Charlesby, A.; Folland, R. *Proc. R. Soc. London, Ser. A* **1979,** 367, (1730), 343-51.
[6] Feio, G.; Buntinx, G.; Cohen-Addad, J. P. *J. Polym. Sci., Part B: Polym. Phys.* **1989,** 27, (1), 1-24.
[7] Feio, G.; Cohen-Addad, J. P. *J. Polym. Sci., Part B: Polym. Phys.* **1988,** 26, (2), 389-412.
[8] Ebengou, R. H.; Cohen-Addad, J. P. *Polymer* **1994,** 35, (14), 2962-9.
[9] Zhang, L; Hansen, E. W.; Helland, I; Hinrichsen, E.; Larsen, Aa.; Roots, J. *Macromolecules* **2009**, 42, (14), 5189-5195
[10] Litvinov, V. M.; Penning, J. P. *Macromol. Chem. Phys.* **2004,** 205, (13), 1721-1734.
[11] Abragam, A., *The Principles of Nuclear Magnetism*. Oxford University press: Oxford, U.K., 1961
[12] Hansen, E. W.; Kristiansen, P. E.; Pedersen, B. *J. Phys. Chem. B* **1998,** 102, (28), 5444-5450.
[13] Kristiansen, P. E.; Hansen, E. W.; Pedersen, B. *J. Phys. Chem. B* **1999,** 103, (18), 3552-3558.
[14] Kristiansen, P. E.; Hansen, E. W.; Pedersen, B. *Polymer* **2000,** 42, (5), 1969-1980.
[15] Hedesiu, C.; Demco, D. E.; Kleppinger, R.; Buda, A. A.; Blümich, B.; Remerie, K.;
[16] Litvinov, V. M. *Polymer* **2007,** 48, (3), 763-777.
[17] Dadayli, D.; Harris, R. K.; Kenwright, A. M.; Say, B. J.; Sunnetcioglu, M. *Polymer* **1994,** 35, 4083-4087.
[18] Uehara, H.; Aoike, T.; Yamanobe, T.; Komoto, T. *Macromolecules* **2002,** 35, (7), 2640-2647.
[19] Brereton, M. G. *The Journal of Chemical Physics* **1991,** 94, 2136.
[20] Brereton, M. G.; Ward, I. M.; Boden, N.; Wright, P. *Macromolecules* **1991,** 24, (8), 2068-2074.
[21] Boden, N. *Chem. Phys. Let*. **1974**, 28 (4), 523 – 525
[22] Boden, N.; Mortimer, M. **1973**, 21 (3), 538 – 540
[23] Mao XA, Holz M. *Appl. Magn. Reson.* 1994; **6**: 529, 2.
[24] Gadan DG, Robinson FNH. *J. Magn. Reson.* 1979; **34**: 449, 3.
[25] Bahlmann EKF, Harris RK, Say BJ. *Magn. Reson. Chem.* 1993; **31**:266, 4.
[26] Vogel AI. *A Text Book of Quantitative Inorganic Analysis*. Longman:London, 1961, 5.
[27] Corine Gerardin,1,2 Mohamed Haouas, Chantal Lorentz and Francis Taulelle; Magnetic Resonance in Chemistry, *Magn. Reson. Chem.* 2000; **38**: 429–435)